Video monitoring of in-channel wood: from flux characterization and prediction to recommendations to equip stations

Zhi Zhang, Hossein Ghaffarian, Bruce Macvicar, Lise Vaudor, Aurélie Antonio, Kristell Michel, Hervé Piégay

Video monitoring of in-channel wood: from flux characterization and prediction to recommendations to equip stations

Zhi Zhang[1], Hossein Ghaffarian[1] *, Bruce MacVicar[2], Lise Vaudor[1], Aurélie Antonio[1], Kristell Michel[1], Hervé Piégay[1]

[1]Univ. Lyon, UMR 5600, Environnement-Ville-Société CNRS, F-69362 Lyon, France

[2]Department of Civil and Environmental Engineering, Univ. Waterloo, Waterloo, Ontario, Canada

* Corresponding author: Tel.: +33(0) 7 69 67 00 50; E-mail: hossein.ghaffarian@ens-lyon.fr

Abstract

Wood flux (piece number per time interval) is a key parameter for understanding wood budgeting, determining the controlling factors, and managing flood risk in a river basin. Quantitative wood flux data is critically needed to improve the understanding of wood dynamics and estimate wood discharge in rivers. In this study, the streamside videography technique was applied to detect wood passage and measure instantaneous rates of wood transport. The goal was to better understand how wood flux responds to flood and wind events and then predict wood flux. In total, one exceptional wind and 7 flood events were monitored on the Ain River, France, and around than 24000 wood pieces were detected visually. It is confirmed that, in general, there is a threshold of wood motion in the river equal to 60% of bankfull discharge. However, in a flood following a windy day, no obvious threshold for wood motion

was observed, confirms that wind is important for the preparation of wood for transport between floods. In two multi-peaks floods, around two-thirds of the total amount of wood was delivered on the first peak, which confirms the importance of the time between floods for predicting wood fluxes. Moreover, we found an empirical relation between wood frequency and wood discharge, which is used to estimate the total wood amount produced by each of the floods. The data set is then used to develop a random forest regression model to predict wood frequency as a function of three input variables that are derived from the flow hydrograph. The model calculates the total wood volume either during day or night based on the video monitoring technique for the first time, which expands its utility for wood budgeting in a watershed. A one-to-one link is then established between the fraction of detected pieces of wood and the dimensionless parameter "$passing\ time \times framerate$", which provides a general guideline for the design of monitoring stations.

Keywords: Fluvial dynamics; Large wood in river; Random forest model; Wind condition; Multi-peaks discharge; Streamside video monitoring.

1. Introduction

Floating wood in rivers, known as driftwood, is a significant component of catchments, notably in forested temperate regions (Wohl, 2013; Ruiz-

Villanueva et al., 2016a). It is delivered to the rivers by a set of processes (landslides, debris flows, blowdown, bank erosion and so on) which vary from upstream to downstream (Nakamura and Swanson, 1993; Montgomery et al., 1996; Abbe and Montgomery, 2003; Gurnell and Petts, 2006). Among different recruitment processes, bank erosion probably delivers most of the large organic material into larger lowland rivers (Keller and Swanson, 1979). These large pieces of wood (i.e. greater than 1 m length and 10 cm diameter) induce variations in hydraulic and sediment dynamics, and contribute to flow resistance and obstructions within the channel (Young, 1991; Gippel, 1995; Shields and Gippel, 1995; Wilcox and Wohl, 2006; Comiti et al., 2008). Especially during a flood, the transport and deposition of large wood pieces represent a potential increase in the destructive power of floods, which increases the potential risks to human populations and infrastructures (Lassettre and Kondolf, 2012; De Cicco et al., 2018; Mazzorana et al., 2018). For instance, a flow obstruction due to wood accumulation can lead to upstream bed aggradation, channel avulsion, and local scouring processes, which can in turn cause embankment or bridge collapse and floodplain inundation (Diehl, 1997; Lyn et al., 2003; Fischer, 2006; Waldner et al., 2007; Mao et al., 2008; Mazzorana et al., 2009; Comiti et al., 2012; Ruiz-Villanueva et al., 2014a). Therefore, quantifying wood inputs, transport, deposition, and budgeting in general is crucial for understanding and

managing wood risk in rivers.

Understanding the variability and the process-scale dynamics which control wood delivery and transport rate is also a critical challenge (Martin and Benda, 2001; Benda et al., 2003; Marcus et al., 2011; Schenk et al., 2014; Boivin et al., 2015). Wood budgeting can be explored at different time scales. The wood recruitment sites are often observed close to the preferential sites of deposition (Schenk et al., 2014; Ravazzolo et al., 2015), but not systematically, as shown along the Isère River, France (Piégay et al., 2017). Some pieces of wood can be transported over very long distances during a single flood (Gurnell et al., 2002; Gurnell, 2012; Comiti et al., 2016; Kramer and Wohl, 2017). Moreover, the amount of wood can be documented at multi-annual and annual time intervals over long time periods by historical data (Seo et al., 2008; Seo and Nakamura, 2009; Ruiz-Villanueva et al., 2014b). Based on this long time scale, however, it is not possible to record continuous series and study wood transport processes during shorter but critical hydrological events such as floods, exceptional wind events, and landslides, which are known to drive wood fluxes in rivers (Lassettre and Kondolf, 2012; Ruiz Villanueva et al., 2014a).

To generate wood input series in shorter time scales, Moulin and Piégay, (2004) used weekly time steps to measure the wood stored in a reservoir. The results quantified the timing and magnitude of Large Wood (LW) export during

flood events in the reservoir and allowed the recruitment and transport processes of LW at the watershed scale to be better understood. Benacchio et al. (2017) monitored wood delivery and calculated wood weight in a reservoir by an automated image processing technique using much finer time intervals (10 min). In addition to the reservoir-based monitoring, Kramer and Wohl, (2014) showed that in high-discharge, low-velocity rivers, the deployment of monitoring cameras with coarse frame rates (≥ 1 min) enables monitoring of LW transport at large spatial and long temporal scales. However, in smaller and steeper rivers the velocity of wood pieces is higher or the field of view is too small such that low frame rate photography cannot provide accurate estimates of wood delivery.

Video monitoring of the water surface can be used to continuously monitor wood flux at a high temporal resolution. Lyn et al. (2003) were the first to apply this technique, using two stream-side video cameras to observe and detect wood accumulation on bridge pier in the Eel River, Unites States. Due to data storage issues, Lyn et al. (2003) downgraded the frame rate to 0.1 fps (frame per second) and applied image compression to the recorded frames through the monitoring period. Such issues were overcome by MacVicar et al. (2009), and MacVicar and Piégay (2012) who established a monitoring station at the Ain River, France, but transferred the full resolution images recorded at 5 fps to

a remote server for analysis. The high quality and frequency of the data, which is likely necessary in high gradient rivers, allowed them to compare LW dynamics with flood hydrograph and develop a quantitative relation between wood and water discharges. Other studies have implemented similar approaches (Boivin et al., 2015; Kramer et al., 2017; Senter et al., 2017; Ruiz-Villanueva et al., 2018; Ghaffarian et al., 2020a) but overall the technique remains undersubscribed and models of the wood flux as a function of the flow hydrograph remain poorly parameterized.

Overall, the success of a particular monitoring station will be determined by issues of wood size and image resolution (MacVicar and Piégay, 2012; Ghaffarian et al., 2020a). Ghaffarian et al. (2020a) monitored floods on the Isère River (France) and demonstrated the generalizability of technique to other rivers along with some limits, constraints, and methodological recommendations. The oblique angle of the camera means that it is particularly important to understand where wood will pass relative to the camera position (Ghaffarian et al., 2020a). Moreover, a problem remains that there are gaps within the data. Such gaps can occur due to the poor visibility in low light or cloudy weather, lost connections where data is transferred to a remote server for storage (Muste et al., 2008; MacVicar et al., 2009; MacVicar and Piégay, 2012; Ghaffarian et al. 2020a), or simply to the time required to extract

information about floating wood from videos. Despite some efforts at automatic extraction (Ali and Tougne, 2009; Lemaire et al., 2014), the procedure to date remains predominantly manual. Improved modeling of wood fluxes as a function of flow hydrographs or other environmental conditions could be an effective strategy to reduce sampling effort and fill in missing data such that wood fluxes could be integrated over time to support wood budgeting in watersheds.

The aim of the current study is to advance the video monitoring technique for wood flux measurement by addressing the following questions: i) is wood transported only above a discharge threshold, and if so, is the threshold a function of antecedent conditions? ii) Can wood flux be modelled as a function of the flood hydrograph? and iii) Can we accurately estimate wood flux from sampling? The analysis uses the database assembled by MacVicar and Piégay (2012) of sampled periods during three floods on the Ain River but significantly adds to this work by performing a complete analysis of the daytime videos from four new flood events and one period with low flow but an exceptional wind condition, which was then followed by a flood event. This much larger database comprises nearly 180 hours of annotated videos or around than 24,000 annotated wood pieces, which substantially expands on the 18 hours and 7800 wood pieces monitored by MacVicar & Piégay (2012). The windy day event with

35-year return period allowed us to address the first research question. A random forest (RF) model was used to answer the second question. Flux and wood measurements from the MacVicar and Piégay (2012) database combined with the data of the present study are used to resolve the third question.

2. Study site

The study site is located on the lower Ain River, a sixth-order piedmont river flowing through a forested corridor in France. The channel is typically single thread with occasional islands, and a wandering system with prominent meander scrolls and cutoff channels (Figure 1.a) (MacVicar et al., 2009). The hydrograph shows a strong seasonal pattern, with low flows in the summer and most of floods occurring between October and April. Bed material sizes are gravel–cobble mix with a median size of 2.5 cm. The unvegetated channel width is 65 m in average at the study site, actively shifting so that significant amount of wood is delivered by bank erosion. Tree species established in the floodplain are a mix of soft and hardwood species dominated by black poplar (Populus nigra) that can reach up to 75 cm in diameter and 25 m in height (MacVicar and Piégay, 2012). Along the study site, wood influx has been estimated over several decades from the analysis of aerial photographs at 18 to 38 m^3/km/yr (Lassettre et al., 2008).

159 Floating wood was counted on the river at Pont de Chazey, where a stream
160 gauge is maintained by a regional authority (Figure 1.b, c). Along the river, the
161 characteristic discharge of 1.5-year return period was $Q_{1.5} = 840$ m^3/s
162 (Ghaffarian et al., 2020a), and at this study site, an estimated bankfull discharge
163 (Q_{bf}) of 530m^3/s was confirmed by visual observation (MacVicar and Piégay,
164 2012). At this point the flow discharge is calculated based on the water elevation
165 measured at the gauging station. These data are available online from 1959 at
166 (www.hydro.eaufrance.fr). Mean daily wind speed is also available from the
167 Meteorological Station of Lyon-Bron (1949-2020) (see Figure 2).

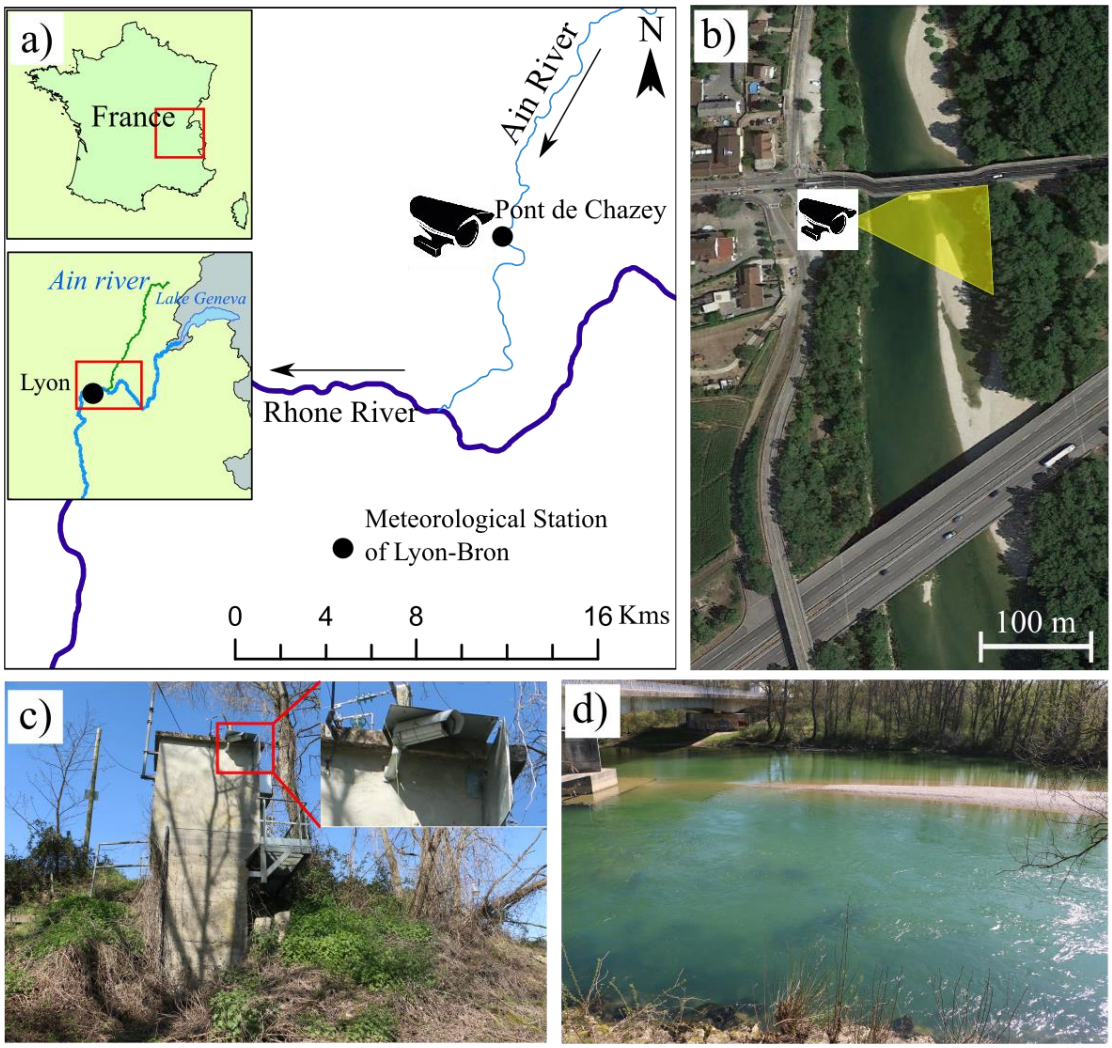

Figure 1. Study site at Pont de Chazey: a) Location of the Ain River course in France and location of the gauging and meteorological stations, b) camera position and its view angle in yellow, c) overview of the gauging station with the camera installation point, d) view of the River channel from the camera

3. Material and Methods

3.1. Stream-side video camera

Wood pieces were monitored at Pont-de-Chazey gauging station using an AXIS P221 Day/Night™ fixed network camera installed in the spring of 2007. Figure 1.d shows the camera field of view on the river surface. The video

173 camera can supply high resolution (HDTV720P) surveillance even in extreme
174 low-light, though not at night time. The camera was located on the side of the
175 river closest to the thalweg to provide a maximum resolution where the majority
176 of wood pieces are observed. The camera elevation is 9.84 m above the base
177 flow surface at a sufficiently wide angle to afford a view of the entire river width
178 during most periods. Ethernet connectivity enables the automatic transfer of
179 recorded videos to a central server where located at CNRS UMR 5600 –
180 Environment Ville et Société, Site of École Normale Supérieure, Lyon, France.
181 Videos were recorded continuously at a maximum frequency of 3 to 5 fps. Data
182 was recorded with this camera from 2007 to 2011 at a resolution of 640×480
183 pixels and from 2012 to 2016 at 768×576 pixels. The first three floods (events
184 F1 to F3) thus have a lower resolution than the final four floods and windy period
185 (events F4 to F7 and W1). At minimum compression, each video segment
186 occupied approximately 94Mb of memory and approximately 15 minutes so that
187 a 4TB hard drive stored approximately one year of video. Flood levels were
188 reviewed every few days and videos of interest were saved for later analysis.

189 ## 3.2. Monitored events

190 In total, 7 flood events were monitored in this study (Table 1). Three flood
191 events from 2007 to 2008 were collected from MacVicar & Piégay (2012),

192 referred to herein as events F1 to F3 (Figure 2.a, red lines). A video camera
193 has been recorded video at this location more or less continuously from 2007.
194 For the current work, four additional flood events between 2012 to 2014 were
195 selected for study and sampling and are referred to as events F4 to F7 (Figure
196 2.a, blue lines). The floods range from 578 m^3/s ($\cong Q_{bf}$) to 1020 m^3/s ($\cong 2Q_{bf}$).
197 Event F7 was selected to assess whether wind has an effect on the wood
198 delivery because it occurred just two days after an exceptional windy day. The
199 windy day occurred on December 24, 2013 and is referred to herein as event
200 W1 (Figure 2.b). The average daily wind speed on this day was 13.6 m/s, which
201 is considered to be a one in 35 year event based on a Gumbel distribution of
202 the over 70 years of record (Yue et al., 1999).

Table 1 Wood sampling statistics at the Pont de Chazey for different events.

Flood periods	Events	Peak flows (m3/s)		Daily wind velocity(m/s)	Analyzed video (hr)	Monitored fraction*	Number of floating woods	
		total	daylight				Rising limb	falling limb
22 to 24-Nov-2007	F1	578	576	6.6	06:15	09%	2800	38
10 to 12-Dec-2007	F2	616	616	6.3	03:45	05%	968	93
10 to 13-Apr-2008	F3	1050	1007	3.8	07:45	08%	3331	584
01 to 07-Jan-2012	F4	808	807	4.9	57:00	34%	3681	1641
15 to 16-Dec-2012	F5	932	821	4.9	17:15	36%	6901	798
01 to 06-Feb-2013	F6	701	701	8.5	56:30	39%	1040	473
24 to 25-Dec-2013	W1	134	134	13.6	08:45	37%	8	-
25 to 27-Dec-2013	F7	600	580	5.6	25:45	36%	1443	43

203 * Monitored fraction = monitored duration / total duration of an event

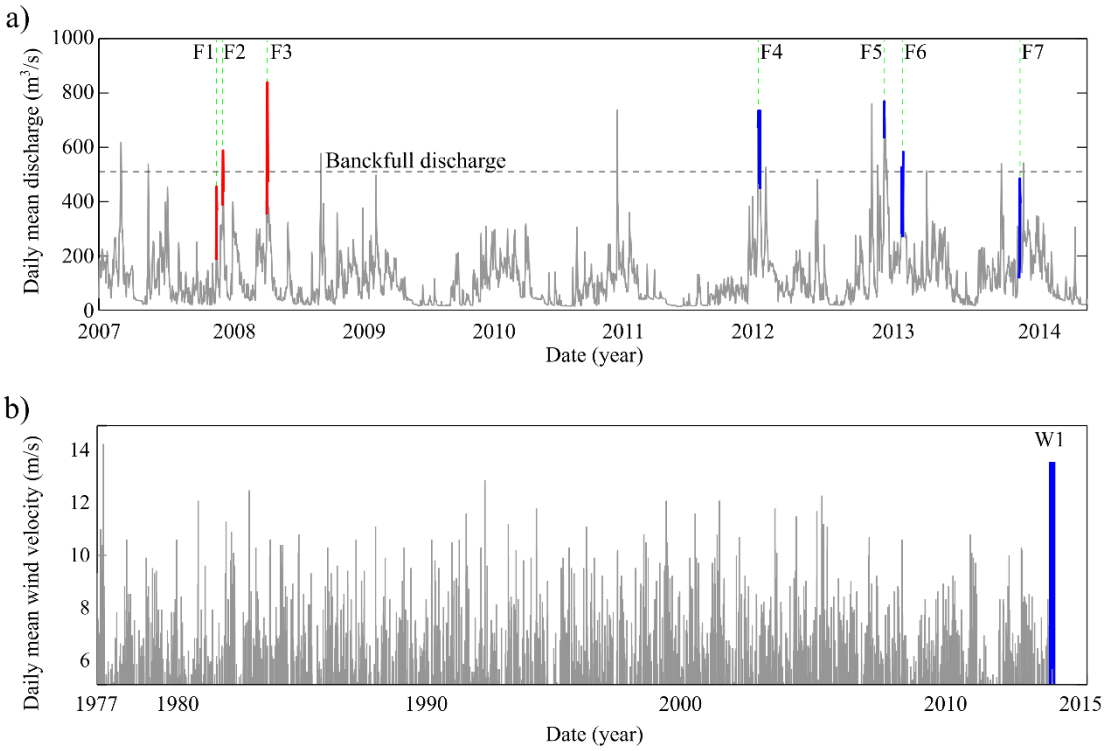

Figure 2. Monitored events a) the daily mean discharge series monitored by MacVicar & Piégay (2012) (red lines) and monitored in this work (blue lines) on the discharge series from 2007 to 2014. b) The daily mean wind velocity series from 1977 to 2013.

3.3. Monitoring process

In total 183 hours of video was analyzed, including 18 hours monitored by MacVicar & Piégay (2012) (Table 1). For this analysis, floating wood was visually detected by an operator and the position of each piece of wood was digitally annotated frame by frame via a graphical user interface.

Two methods were applied for event monitoring: (i) 15-minute monitoring intervals for events F1 to F3; and (ii) continuous monitoring for events F4 to F7 and W1. In the first approach, applied by MacVicar and Piégay (2012), a 15-minute video segment was monitored for each daytime hour (e.g. from 8:30 to

8:45, 9:30 to 9:45, etc. to ~5:30) and, by multiplying the number of detected pieces by four, the wood flux per hour was extrapolated to be compared with other studies. A problem with this sampling strategy was noted by Ghaffarian et al. (2020a), who showed that a 15 min interval may not be sufficient to reliably estimate the hourly wood flux due to short term variability. For this reason, all daytime periods were monitored by an operator for the flood events added as part of the current analysis.

By extracting the detection time for each piece of wood (indicated on top of each frame, see Figure 4.a), wood flux was calculated as the number of wood pieces within a time interval. In the current study, an hour time interval was selected to model the wood fluxes through the flood events (sections 4.1, and 4.2), again for the reasons highlighted by Ghaffarian et al. (2020a). One and 10-minute time intervals were used for analysis in section 4.3 to assess the importance of shorter-term pulses on overall wood fluxes.

3.4. Observer bias

The analyzed events in this work are based on two different operators (MacVicar and Zhang). During the detection process, the operator bias can play a role in the quantity of wood fluxes. To check this effect, 13 segments of 15-minute videos from events F1 to F3 were selected and wood was detected by

232 both operators following the process used by Ghaffarian et al. (2020a). These
233 video segments were selected such that they cover different light conditions
234 (e.g. sunshine or cloudy weather or different day times) to evaluate the operator
235 visions in this range of conditions. Also, the amount of wood pieces varies
236 greatly among the videos (from 0 to more than 300 pieces), which allowed us
237 to assess whether bias was affected by wood frequency. Overall, there was a
238 ~7% difference in wood flux estimates between the two observers, with most
239 discrepancies occurring when many small wood pieces pass through the image
240 within a short time interval.

241 ## 3.5. Modeling wood flux

242 A random forest (RF) non-linear regression algorithm was applied to model
243 the link between wood flux and flow discharge in this study. It produces multiple
244 decision trees (here, 500), each of which is trained on a randomly selected
245 subset of the data (in-bag portion) while the remaining subset is used to test
246 the regression and assess its performance (out-of-bag portion)(Breiman, 2001;
247 Hastie et al., 2009; Belgiu and Drăguţ, 2016). The RF error corresponds to the
248 residual sums of squares averaged across all the out-of-bag portions of the
249 regression trees. The importance of a variable in the RF model can be assessed
250 through a score that corresponds to the total decrease in error due to splits on

that particular variable, averaged across all trees (Breiman, 2001).

For the current study, the response variable was the wood flux and the predictor variables were all derived from the flow time series. We considered three predictors that could influence the wood flux during flood including: (i) flow discharge $Q(t)$, (ii) the time elapsed since the last time that Q was higher or equal to $Q(t)$, known as T_Q, and (iii) the gradient of discharge over a time lag (5 min) dQ/dt. The application of these predictors in the model is presented in the results (section 4.2). Due to gaps in sampling (e.g., during night time), periods where the time interval between two consecutive detections exceeded 10 hr were removed from the data. In cases when several pieces of wood were annotated in the same image frame, we assume a time interval of 0.5 s between wood pieces.

The RF and all related data-wrangling were carried out using the R software (R Core Team, 2019) and the Random Forest package (Liaw and Wiener, 2002). The random forest consisted of a default number of trees set to 500 and the sampling of in-bag/out-of-bag samples was made with replacement. The R notebook gathering all RF-related commands is available from https://github.com/lvaudor/wood_flux.

3.6. From wood flux to wood discharge

In the study by MacVicar and Piégay (2012), wood discharge was calculated as m^3/s by estimating the length and diameter of all detected floating wood pieces. This process is time consuming, and a decision was made for the current study that, rather than completing the size measurements, the wood pieces would only be counted for floods F4 through F7. The wood count allowed the calculation of the wood flux as a frequency (pieces/minute). This approach was justified by considering Figure 3, which shows that there was a strong correlation between wood flux and wood discharge for the 15 min video segments (see section 3.3) sampled by MacVicar and Piégay (2012) for F1, F2 and F3 ($R^2 = 0.83$). This strong relation gives confidence that wood discharge and the total wood volume can be reliably estimated from the wood flux to allow comparison with other studies and models of the wood budget. Extrapolating this relation for other rivers would be an open question that can be the objective of future comparative works.

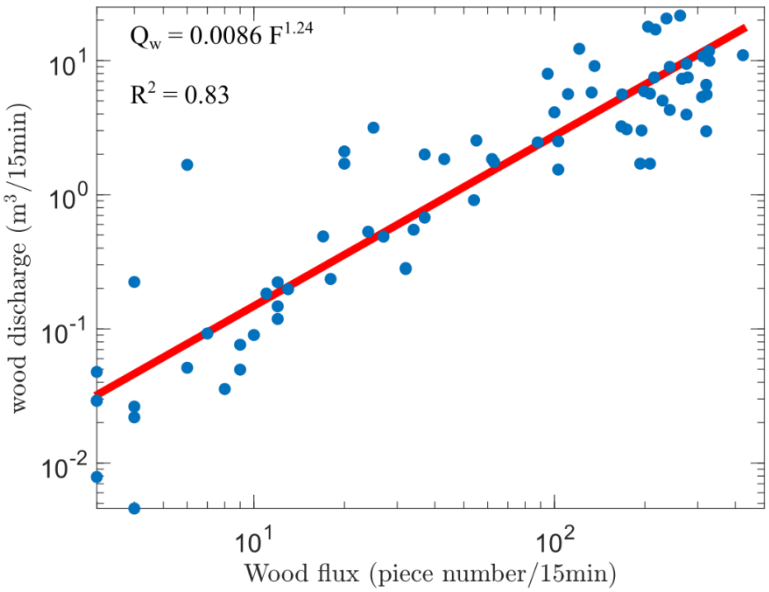

Figure 3. Wood discharge as a function of wood flux

3.7. Sampling strategy

Taking advantage of high temporal resolution videography, it is possible to capture all variations of wood flux during a critical event, while low frame rate photography can be used to detect only a fraction of wood fluxes in the river. To understand the link between the detected wood fluxes and the frame rate, here the concept of passing time (PT) is introduced as the time that one piece of wood passes through the camera field of view. As the camera has a large oblique view, PT varies a lot from the foreground to background (right side of Figure 4.a). Therefore, to measure PT, the position where most of wood pieces' pass is used. As it is seen in the left side of Figure 4.a, more than 75% of wood pieces pass from 150 to 250 pixels on j direction. The passing time at this region is around $PT \cong 5s$ (right side of Figure 4.a). Theoretically, in one snapshot of

296 the camera corresponds to time t_i, this object can be detectable from $t_i - \frac{PT}{2}$ to

297 $t_i + \frac{PT}{2}$.

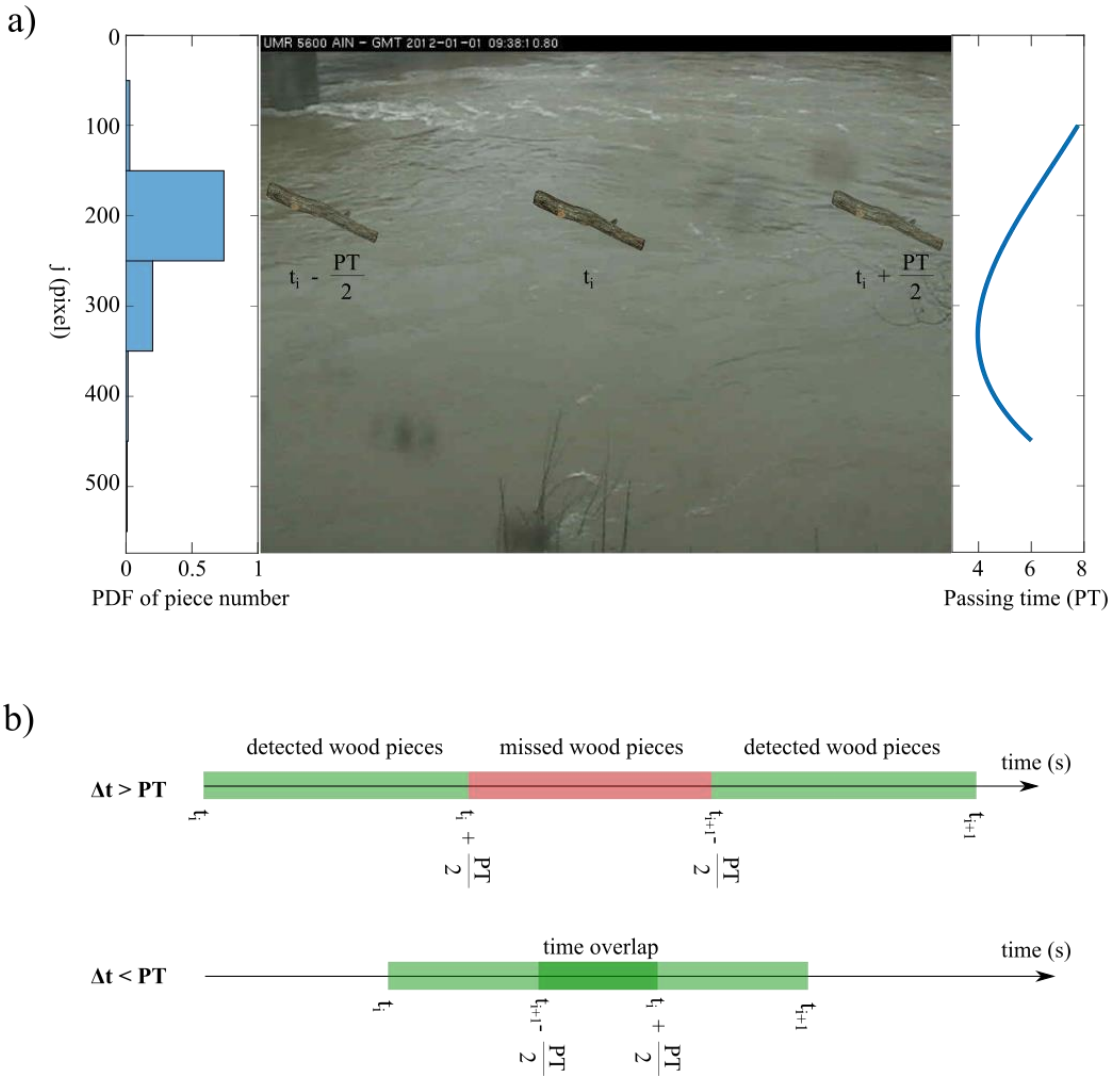

Figure 4. a) wood flux position on video frame b) link between video time laps Δt and the passing time *PT*

298 By introducing the frame rate (of frame per second fps) as one over the

299 time between two consecutive frames ($fps = \frac{1}{\Delta t} = \frac{1}{t_{i+1} - t_i}$), all the objects that

300 pass from $t_i - \frac{PT}{2}$ to $t_i + \frac{PT}{2}$ or from $t_{i+1} - \frac{PT}{2}$ to $t_{i+1} + \frac{PT}{2}$ can be detected by the

301 observer at each camera snapshot (see Figure 4.b). Consequently, if $\Delta t > PT$,

302 there can be some pieces that cannot be detected by the camera (red region in
303 Figure 4.b, top), while if $\Delta t < PT$, we can be sure that no wood piece is missed
304 between each pair of frames (Figure 4.b, bottom). Therefore, the fraction of the
305 detected wood pieces can be defined as the ratio between detected wood
306 pieces in the green region in Figure 4.b and the summation of detected (green
307 region) and missed pieces (red region). To study the link between the frame
308 rate and the fraction of detected wood pieces, all detections in Table 1 were
309 used. Knowing $\Delta t = 0.2s$ $(5\ fps)$ and $PT \cong 5\ s$ on the Ain river, we know that
310 $\Delta t \gg PT$ means that there is enough overlap between each pair of frames (the
311 condition presented in the bottom of Figure 4.b) and wood can be detected.
312 Note that while PT changes both with discharge conditions and the transvers
313 position of detection, the value $PT \cong 5\ s$ is a rough value for estimating the ratio
314 between frame rate and passing time. Moreover, the 'detectability' of wood
315 pieces does not account for wood that is not clearly visible in the frame (for e.g.
316 small pieces far from the camera), which is a separate issue related to image
317 resolution and camera angle/position. Given the detection time for each piece
318 of wood (as recorded on top of each frame - see Figure 4.a), the effect of the
319 frame rate on the number of detectable wood pieces was assessed by artificially
320 changing the frame rate from 0.001 to $5\ fps$ $(0.2s < \Delta t < 1000s)$. Results are
321 presented in section 4.3.

4. Results

4.1. Estimate of wood fluxes during critical events

Overall, the results show 3-stages of (i) rising from a threshold of motion, (ii) high but flat at discharges above the bankfull, and then (iii) around one order of magnitude lower on the falling limb (Figure 5 and Table 1). In Figure 5 the blue scatters from the new events are quite consistent with the events in red from MacVicar and Piégay (2012) which validates the sampling technique.

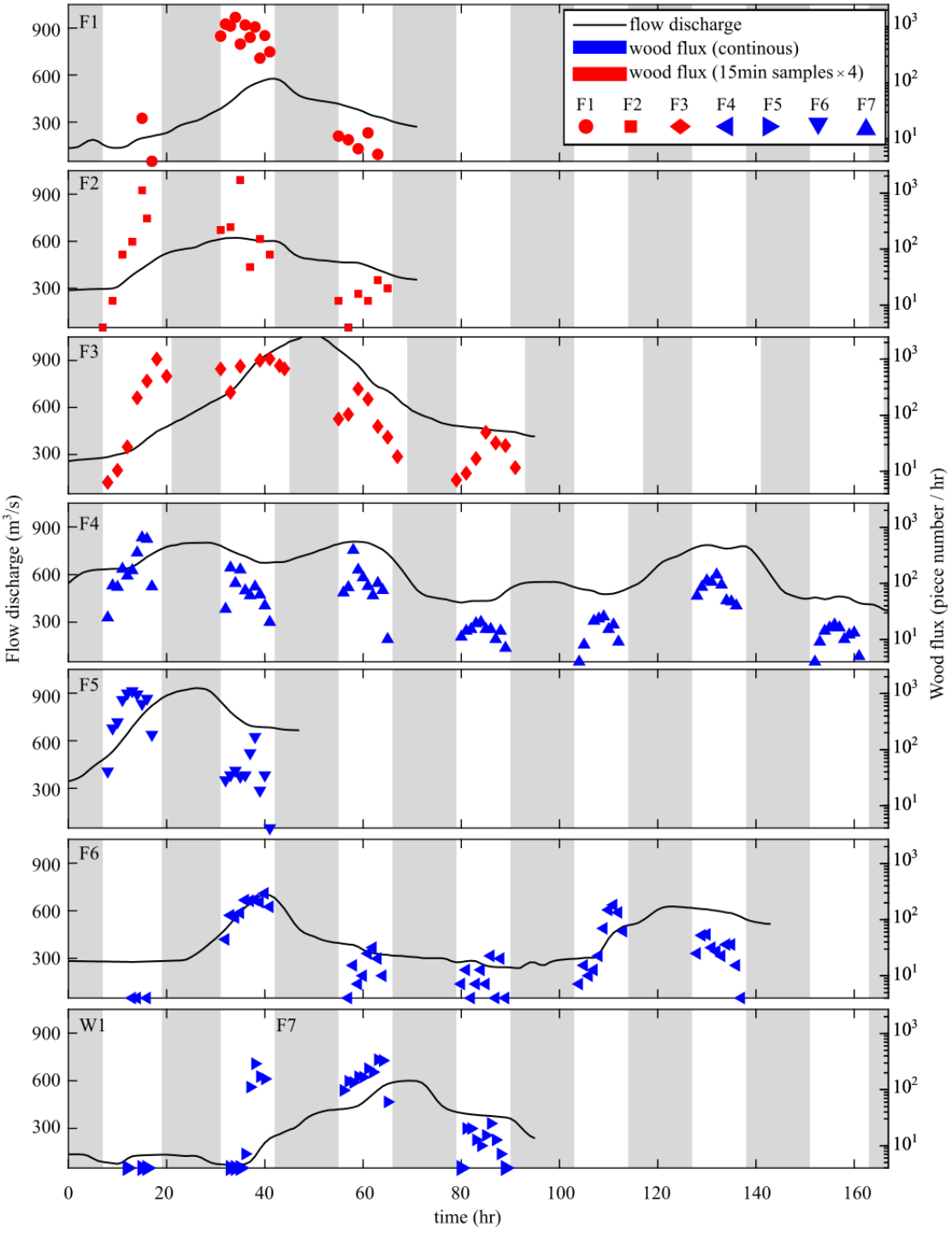

Figure 5. Comparison between wood flux based on sampling (red) and continuous (blue) monitoring and flood hydrograph (black line). The gray boxes show the night time when video monitoring was impossible. Different symbol shapes show different events and are consistent with some of the next figures.

329 During the exceptional windy day (W1 from 8 to 17 hr) almost no wood was

330 detected on the river (Table 1). This means that the wood flux is only observed
331 during flood events. As it is seen in Figure 5 in all cases but F7, there are almost
332 no wood pieces in the river for flow discharge less than ~300 m^3/s. In the case
333 of the flood event F7 following W1 (the exceptional wind event), however, the
334 threshold appears to be much lower or non-existent. For this event only, the
335 wood flux increases immediately following the increase in flow discharge, which
336 demonstrates the potential effect of W1, not in terms of transport of floating
337 wood downstream, but in the wood transfer from the river banks to the channel
338 where it can be readily mobilized in the subsequent flood.

339 In Figure 5, events F4 and F6 are characterized by multi-peak hydrographs.
340 Event F4, for example, is characterized by three peaks with similar discharges
341 (Table 2), during which 3098, 1134 and 839 pieces of wood were observed
342 respectively in the first to third peaks. Event F6 is characterized by two slightly
343 lower peaks, and 995 and 427 pieces of wood were observed in two peaks,
344 respectively (Table 2). Despite some differences in the timing of the floods with
345 respect to daylight hours, these results do indicate that around two-thirds of the
346 wood are mobilized in the first peak of a multi-peak flood. As the number of
347 peaks increases, it also appears that the amount of transported wood
348 progressively decreases.

Table 2 Wood flux in multi peak floods F4 and F6

Flood event	F4.1(Peak1)	F4.2(Peak2)	F4.3(Peak3)	F6.1(Peak1)	F6.2(Peak2)
Q_{max} (m^3/s)	801	808	786	701	627
Pieces number	3098	1134	839	995	427
Fraction*	61%	23%	16%	71%	29%
Flux on rising limb (num/hr)	268	211	82	97	35

* Fraction = piece number during one peak / total piece number during an event.

4.2. Predicting wood fluxes from the flow hydrograph

As described in section 3.5, three predictors derived from the flow hydrograph that were thought to influence the wood flux during the flood were used to develop a RF model. Figure 6 shows the link between (i) flow discharge ($Q(t)$) (Figure 6.a), (ii) the gradient of discharge over 5 min time lag (dQ/dt) (Figure 6.b), and (iii) the time elapsed since the last time that Q was higher or equal to $Q(t)$ (T_Q) (Figure 6.c) from one hand, and the wood flux from the other hand. Regarding the first predictor, as is seen in Figure 6.a, $Q(t)$ has a non-linear positive relationship with the wood flux. Wood flux starts to respond to $Q(t)$ from a threshold almost equal to 450 m^3/s and reaches its maximum value at around 850 m^3/s. These values agree with observed values in Figure 5. For the second predictor, a comparison between positive and negative values of dQ/dt (rising and falling limb) in Figure 6.b shows that while there is a strong effect of flow discharge gradient on the rising limb, there is almost no effect of the discharge gradient on the falling limb. Finally, as seen in Figure 6.c even with a strong initial fluctuation, the wood flux increases with increasing inter-

366 flood time.

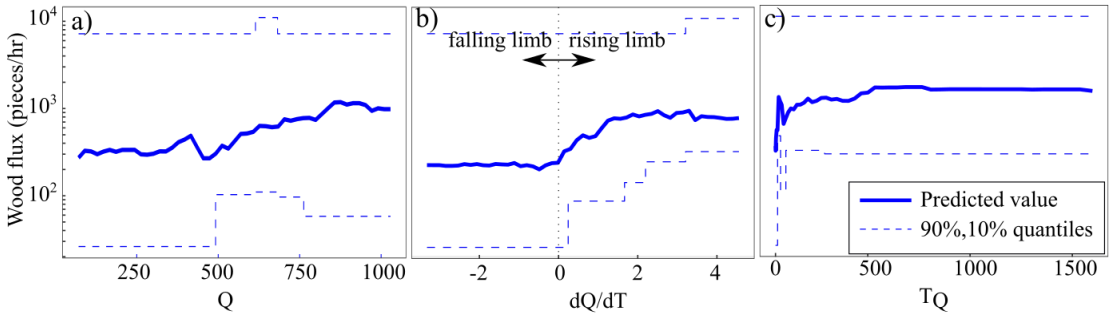

Figure 6 Predicted value of wood flux (in blue) as a function of a) flow discharge Q (m3/s), b) discharge gradient dQ/dt (m3/s/1hr) and c) the time elapsed since the last time that Q was higher or equal to $Q(t)$, T_Q (days). Dashed lines indicate the 90% and 10% quantiles of the data.

367 Figure 7 compares the observed and the modelled wood fluxes time series
368 (aggregated by hour) for continuous (blue) and sampled (red) videos. The clear
369 strength of the model is that the modelled flux is continuous and provides
370 information during the night and other gaps in the wood sampling database. In
371 terms of performance, the number of trees in the RF model (500) was sufficient
372 to show a convergence on the minimum error possible from this data set. The
373 final average R^2 for the out-of-bag portion across all trees was 49.5%. When
374 carrying out cross-validation for the RF as a whole (with 80% of the data
375 randomly sampled –without replacement- as the training set and 20% as the
376 test set) the R^2 for training set was also 49.5% on average across all trees for
377 the training set (estimated on the out-of-bag data) and 69.8% on the test set.
378 The most important predictor is T_Q (responsible for 41% of the total increase in

379 node purity –as measured by the residual sum of squares-), followed by Q (32%)
380 and dQ/dt (27%). To assess the efficiency of the model more objectively,
381 Figure 8 compares observed and modelled data on the rising and falling limbs
382 of the hydrograph at each event. Each data point represents the sum of wood
383 flux values over the entire limb of the flood during the daylight. As shown, the
384 model predicts the observations with a precision estimated to about 95%.

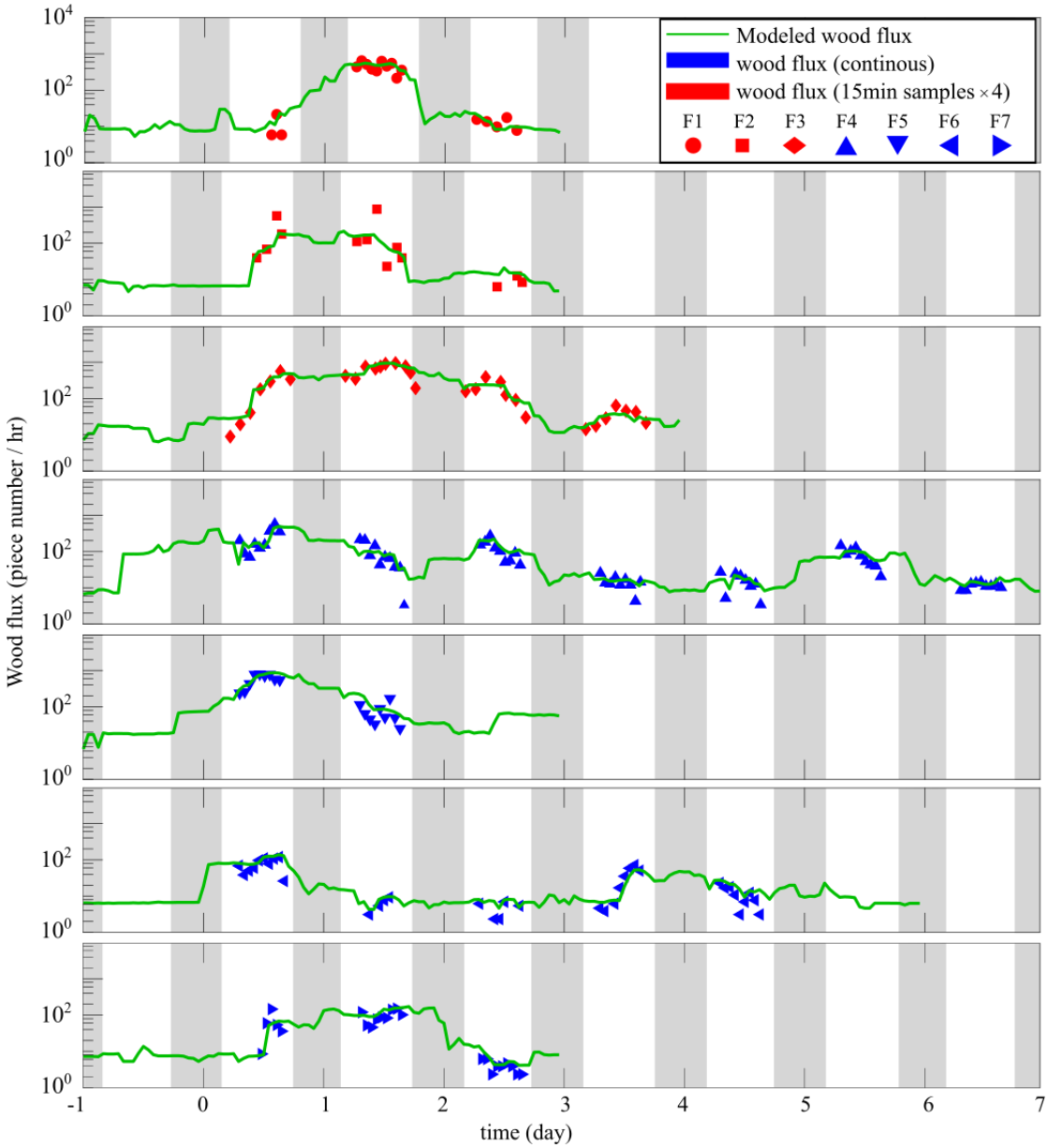

Figure 7. Wood fluxes based on continuous (blue) and sampled (red) videos and

modelled wood fluxes (green line) using RF model as a function of time.

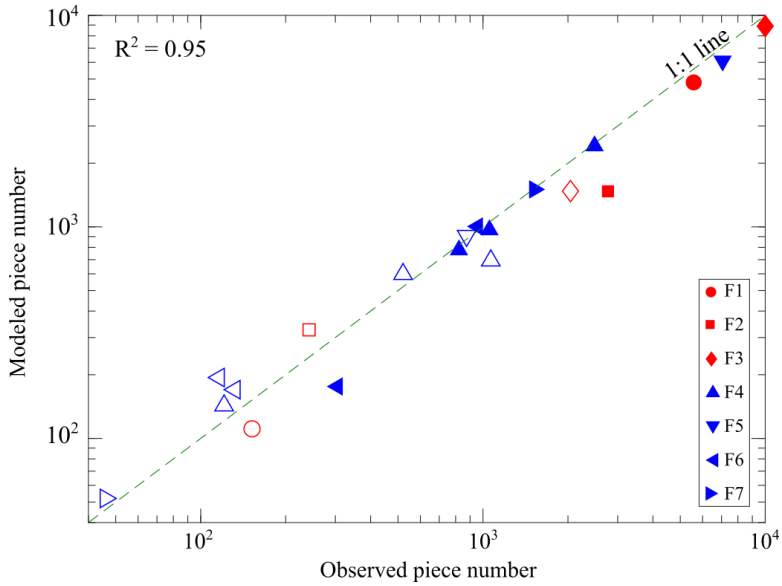

Figure 8. Comparison between observed and modelled piece number: filled and empty scatters show data on the rising and falling limbs of the hydrograph, respectively. Data are compared with a 1:1 line. There are 3 points for F4 and 2 points for F6 due to multiple peak floods.

385 Based on the field observations and the RF modelled wood fluxes, it is
386 possible to check both the wood mobility during the night and the critical
387 threshold of motion. The critical threshold of motion is defined by the discharge
388 which initiates the mobility of wood flux on the rising limb of the flood. Moreover,
389 to be able to compare the wood volume in two different approaches
390 (observation and model) the process described in section 3.6 was used.

391 The new phenomenon that is observed here is the exceptional windy day
392 W1 with low flow ($Q < 0.18Q_{bf}$) which is followed by a flood ($Q > Q_{bf}$) F7.
393 During this wind event, almost no wood flux was detected at the video
394 monitoring station (only 2 m^3). In the subsequent flood, however, the threshold

of wood motion was approximately $0.2Q_{bf}$ (95 m^3/s), which is significantly less than the threshold at $0.6Q_{bf}$ for the other flood events (Table 3). Note that in some cases the thresholds occurred during the night, in which case the presented values are the modelled results.

Table 3 Wood volume and threshold of wood motion, modelled (M) or observed (O).

Event	F1	F2	F3	F4	F5	F6	W1	F7
Modelled wood volume* (m^3)	218.69	84.95	680.68	347.08	412.54	52.81	1.88	77.11
Observed wood volume (m^3)	88.75	32.41	120.01	118.29	235.05	26.12	0.03	29.36
Threshold (m^3/s)	275	300	300	300	350	356	<95	95
Modelled/Observed	M	O	O	M	M	M	O	O

* Modeled wood volume includes volume during both day and night time.

4.3. Validation optimal wood flux estimate from sampling

The temporal resolution of video monitoring plays a significant role on the quantity of monitored data. By introducing the passing time PT and the frame rate $1/\Delta t$ (as shown in Figure 4, section 3.7), Figure 9 shows the link between the fraction of detected wood fluxes as a function of the dimensionless parameter $PT/\Delta t$. As a note, this figure shows the numerical link between frame rate, passing time, and the fraction of detected objects, while in practice other sources of uncertainty may be important as discussed in section 5. From the Figure 9, it is nevertheless clear that frame rates less than the passing time are necessary for a full census monitoring of transported wood.

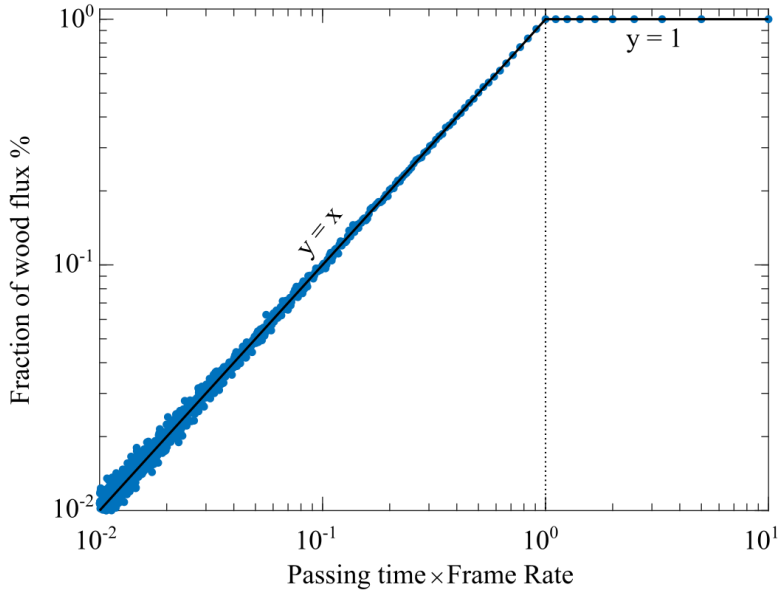

Figure 9. Effect of frame rate and passing time on the fraction of detected wood pieces.

In addition to the fraction of detected wood pieces, the time interval can affect the detection of some short events like wood pulses, defined qualitatively as the delivery of large amount of wood in a short time period (on the order of minutes). Figure 10.a is an example of detected pulses in the event F4 where the wood flux is presented on 1 min intervals. As shown, short term pulses with fluxes much higher than the hourly average are common. To check the quality of detection for such short events, Figure 10.b shows one day detection of wood with one pulse at 10am 3th Jan 2012. As it is seen, the possibility to detect wood pulse decreases by decreasing frame rate (from red to blue) when considering the flow conditions observed on the Ain River station.

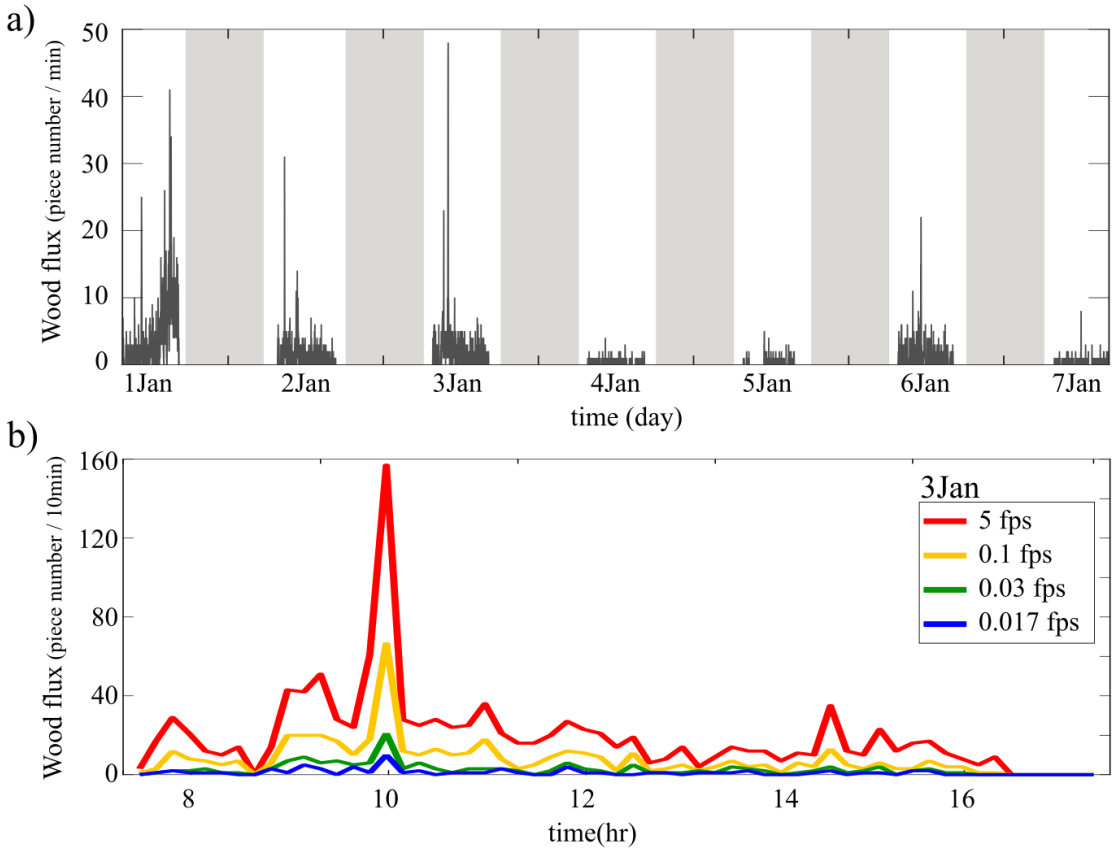

Figure 10. a) Wood fluxes as observed in 1-minute intervals. Beside short fluctuations of wood flux, pulses of wood can be defined qualitatively as the delivery of large amount of wood in a short period of time. The gray boxes show the night time when video monitoring was impossible. b) Effect of the temporal resolution on detecting short time events (a wood pulse).

5. Discussions and conclusions

5.1. The link between flow hydrographs and wood fluxes

Our observations confirm that most of the wood pieces are mobilized on the rising limb of the hydrograph than the falling limb following MacVicar and Piégay, (2012), Kramer and Wohl, (2014) and Ghaffarian et al. (2020a). The peak in wood flux is generally reached before the flood peak. These observations

426 demonstrate some hysteresis of water discharge that agrees with MacVicar and
427 Piégay (2012) and Ghaffarian et al. (2020a), who state that the peak discharge
428 and the peak of wood flux do not occur simultaneously and normally wood
429 transport rate decreased before the peak of hydrograph. This result has also
430 been confirmed by the model of Ruiz-Villanueva et al. (2016a). They show that
431 wood flux increases with discharge until it attains an upper threshold or tipping
432 point and then decreases or increases much more slowly.

433 A flood hydrograph can be characterized by several peaks. We observed
434 that the second or the third peaks, even when more intense, carry lower
435 amounts of wood (Table 2). This result agrees with Moulin and Piégay (2004)
436 who indicate that the deposited wood on channel edges from the last event
437 (such as: flood, wind and ice (Boivin et al., 2015)) is transmitted by the first
438 rising of water depth. In addition, Kramer et al. (2017) showed that the
439 sequence of peaks, flow discharge and the shape of hydrograph can influence
440 the amount of wood during a flood. As it is seen in the Table 2, more than 60%
441 of wood pieces are carried out on the first peak and then, only 30~40% of wood
442 pieces are observed. This decrease in wood flux by increasing the peaks of the
443 flood can be related to the rate of bank erosion and by the initial conditions of
444 the channel in term of wood delivery by external drivers such as wind, ice and
445 tree mortality. The first peak of hydrograph washes most of the wood available

within the channel and its edges and prepared over the previous no-flood period, only depositing few wood pieces on channel edges as new recruited material from bank erosion. There is also less green wood which is recruited by a new bank erosion process in the next peaks of hydrograph because the shear stress is not as high as the one observed during the first peak along the eroded bank because channel is now wider and not yet adjusted through vegetation encroachment on the accretion area on the other side of the channel.

Moulin and Piégay (2004) show that the wood flux during flood events is not independent from previous floods. For comparison we can look at events F5 and F6, which occur one year and two months after a big flood event respectively. F5 has 5 times the wood flux of F6, which indicates that more wood was available for F5, likely from smaller events and external drivers within the inter-flood period that introduced wood pieces that are then flushed by F5. Therefore, wood flux can be a combination of fresh material as well as in-channel stored and newly recruited material. These internal mechanisms are fairly important as shown by the RF results which showed T_Q is the most important predictor. This agrees with Ruiz-Villanueva et al. (2016a) which shows that a lot of wood material stored upstream of a dam spent some time as deposited wood in the river before being delivered to the reservoir.

This is also potentially confirmed by observations done during and after the

466 exceptional wind event which played a critical role on wood delivery. In the
467 current study, for example, some of the wood transported in event F7 was likely
468 provided by W1. This result indicates that during a windy period, pieces of wood
469 are recruited into the river, but there is not enough flow velocity and depth for
470 moving these wood pieces further downstream. Later, when water depth and
471 the wetted area of the river increases, the river flow is able to begin to move
472 these wood pieces relatively easily, i.e. at thresholds less than the threshold of
473 wood motion where exceptional wind events did not occur ($0.6Q_{bf}$). Therefore,
474 while the wind is not directly related to the mobility of wood, it can decrease the
475 threshold of motion and prepare wood material to be exported during the next
476 flood playing a significant role to explain the T_Q contribution. This result is the
477 first example in which we were able to detect an effective role of a potential
478 driver within the upper catchment.

479 A practical recommendation that derives from this improved understanding
480 of wood mobilization is that recording can largely be initiated strictly as a result
481 of flow discharge, for example by setting the camera to record only when Q
482 exceeds $0.6Q_{bf}$, which would minimize the storage needs for videos while
483 capturing by far the largest contributions to the annual wood flux. However, the
484 effect of wind that causes wood transport at lower discharges needs to be more
485 deeply explored using longer time series to explain wood flux differences

between floods. This factor could be then added in the RF model if applied on a longer time series with more flood events.

5.2. Continuous modeling of wood fluxes

As it is described in section 3.5, a Random Forest model was used to model wood pieces during the night, when no wood is visible in relation to three predictors derived from a continuous flow hydrograph. Figure 6 shows that these three predictors and wood flux are correlated. Regarding the first predictor $Q(t)$, MacVicar & Piégay, (2012) and Ghaffarian et al. (2020a), both showed that the wood flux is expected to have a non-linear positive relationship with flow discharge, which was reflected in Figure 6.a. Also, dQ/dt, as the second predictor, captures the effect of variations in water discharge on wood recruitment during rising (positive values) vs falling (negative values) limb. The direct link between dQ/dt and wood flux on the rising limb in Figure 6.b suggests that increasing the water level during the rising limb of the flow hydrograph can be considered as one of the key parameters on wood delivery in rivers.

The third predictor, T_Q was introduced to account for wood input processes between floods. The RF modelling showed that this parameter was the most important predictor of wood flux for this data set, which is surprising given the

505 primary focus on water level and rate of increase in previous work. Kramer et
506 al. (2017) do show the strong effect of time between floods on the pulses of
507 wood exported from the Slave River, Canada. Ghaffarian et al. (2020a) also
508 show that time between floods has a logarithmic relation with wood flux, which
509 is confirmed in Figure 6.c. The wood input processes are not modelled explicitly,
510 however, and greater understanding at the process scale may help to develop
511 models that are more readily adapted for different catchments. In conclusion,
512 the good performance of the three predictors (Q, T_Q and dQ/dt) RF model
513 shows that it can be used to predict the wood fluxes on the Ain River given a
514 flow hydrograph. Similar models could be developed in other catchments for
515 comparison and a more general result.

516 ## 5.3. Selecting an optimized frame rate

517 A reduced frame rate may reduce wood detection rates so that considering
518 frame rate and passing time is critical to optimize the wood detection. Because
519 reducing the frame rate is a rational strategy to reduce recording costs, there is
520 always a trade-off between the temporal resolution of video (and computer
521 storage capacity) and the recording and post-processing costs to carefully
522 consider. For example, at a frame rate of twice the passing time, only about
523 50% of the passing wood pieces are detectable (Figure 9). Figure 11, (solid

lines) shows the fraction of detected fluxes as a function of passing time PT based on the model presented in Figure 9 for the frame rates used by three different studies: (i) Kramer and Wohl, (2014) on the Slave River, Canada with 0.033 fps, (ii) Ghaffarian et al. (2020a) on the Isère River, France with 1 fps and (iii) MacVicar and Piégay (2012) and this study on the Ain River, France with 5 fps. The link between PT and the fraction of detected fluxes is a function of camera frame rate on each river. This function which is presented as solid lines in Figure 11, is compared with the estimated passing time on each river (dashed lines). For all cases an increase of PT results in an exponential increase of the fraction of detected wood pieces, which is governed by Δt (Figure 9). This exponential relation is a strength for the model because the fraction of detected wood pieces is not so sensitive to the PT, so we do not need to select an exact Δt and it can be varied in the same order of magnitude.

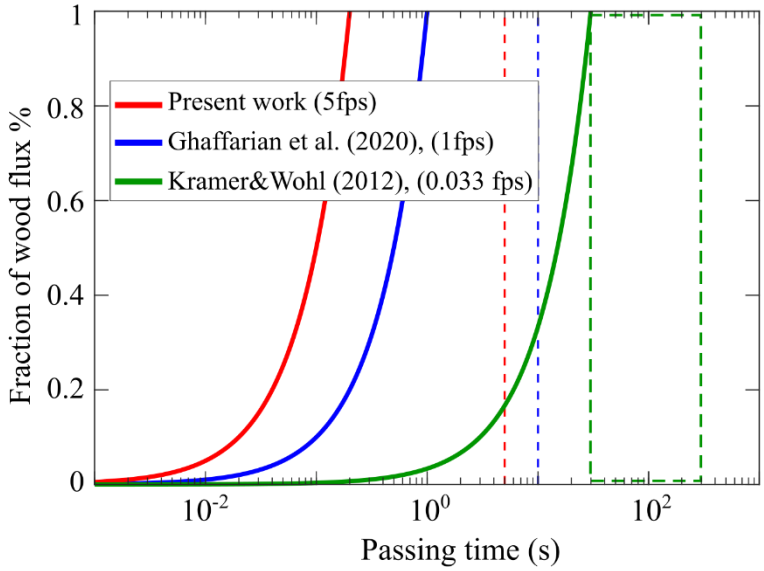

Figure 11. Fraction of detected woods based on passing time in different rivers.

Dashed lines show the estimated passing time on each river, green the Slave, blue, the Isère and red the Ain rivers respectively.

537 The three studies vary in the fraction of detected wood due to differences
538 in passing time and frame rate. As shown by Ghaffarian et al. (2020a), the
539 passing wood in the monitored sections in both the Ain and Isère Rivers was
540 highly concentrated within a relatively narrow band of the wetted width. As a
541 result, PT was relatively consistent, with a mode of ~ 5 and 10 s in the
542 respective channels (Figure 11, red and blue dashed lines respectively). In
543 contrast, wood on the Slave River was laterally dispersed across the channel
544 from 20 to 100 m (Kramer and Wohl, 2014) and the flow velocity on the Slave
545 River was relatively low (~1/10th the velocity in Ain and Isère Rivers). Large
546 variation in transport distance and low flow velocity both result in huge variation
547 of PT on this river, roughly from $30s$ to $120s$ (Figure 11, green dashed line). As
548 a result, all wood on the Isère and Ain Rivers using the parameters as described
549 by Ghaffarian et al. (2020a), MacVicar and Piégay (2012) and this work. In
550 contrast, on the Slave River the frame rate is $0.033\ fps$ ($\Delta t = 30s$) and $30s <$
551 $PT < 120s$, as shown in Figure 11 (green dashed line), which indicates that not
552 all the wood was detectable.

553 To discuss the Slave River, it is necessary to distinguish between time-
554 lapse photography and videography techniques. Although time-lapse

555 photography and video monitoring use the same approach (photos are taken
556 per unit time), time-lapse photography is intended to subsample wood flux and
557 there is no expectation that all of the wood is recorded. Missing data is
558 expected and planned for. In contrast, video capture is a method to store and
559 record the entire sample of wood flux and each piece of wood is expected to be
560 captured in multiple frames. The condition near $PT \cong \Delta T$, however, represents
561 a transition zone between time-lapse photography and video monitoring where
562 errors may occur. For example, at this frame rate a given piece of wood may
563 be seen once or maybe a few times within the series of captured frames. If it
564 appears more than once the wood may be double-counted, particularly where
565 visibility is poor, the wood changes in orientation or submergence, or changes
566 in the surface reflections and lighting can fool the operator such that they flag
567 the same piece of wood more than once. Higher frame rates will decrease the
568 differences between frames and the likelihood of double-counting along with it.
569 Lower frame rates will remove the possibility of double counting and ensure that
570 the monitoring captures only a sub-set of the passing wood, which can then be
571 corrected for missing data as is expected for this technique. The Slave River
572 study is thus within the transition zone from time-lapse photography to video
573 monitoring where double-counting remains a possibility.

574 As a further practical recommendation, it is important to select an

appropriate frame rate for the camera based on a good estimate of velocity conditions in space and in time. Moreover, if the pattern of pulses or the source of wood pieces is important, the frame rate should be large enough to continuously detect wood pieces, while if there is a limitation on storage or long-term data is needed it is recommended to decrease frame rate and adopt a time-lapse subsampling strategy but considering a continuous acquisition window of at least 30 minutes as shown by Ghaffarian et al. (2020a) to minimize uncertainties in wood frequency estimate due to short term pulses.

5.4. Wood pulses

During our observations, it is seen that in some cases the wood flux is mobilized in a sharp pulse, which is typically accompanied by some large pieces of wood that may be recent tree falls or a jam suddenly mobilized. The clarity of these pulses in the video monitoring technique directly relates to the temporal resolution of the camera (Figure 10.b). Moreover, such pulses are fully detectable only if continuous monitoring approach is applied. The difference between continuous monitoring and sampling is visible in Figure 5 where the blue scatters show more consistency through each day, which likely is due to the continuous sampling method (samples were the total per hour rather than 15 min multiplied by 4 as for the red scatters).

It can be hypothesized that wood pulses are the result of either localized or distant wood delivery. Presumably, in such cases of local mobilization, the source of wood could be close to the camera and so the wood would be tightly grouped in time. Such pulses are observed at the Ain River location, where large wood with visible leaves and root wads are followed by large numbers of smaller pieces of wood. In this case the pulse was attributed to local bank erosion or the sudden mobilization of a wood jam. In contrast, the source of wood could be far upstream from the camera, which dispersed wood in transport tending to agglomerate over longer distances. Such a process of 'rafting' or 'clumping' has been observed in the lab and field (Braudrick et al., 1997; Kramer et al., 2017). Therefore, due to the dissipation, the wood pulse spreads out during transport in long distances. The pulses at the camera location would therefore be very spread out and come more or less regularly, which could mean that the inputs are random or that the distribution has been randomized by dissipation during transport. On the falling limb, despite the bank erosion due to the decrease in the soil pore pressure, the flow might not be enough to transport this wood. Also, some wood pieces have already been deposited in the highest possible locations with other wood jams on the upstream floodplain (Ruiz-Villanueva et al., 2016b; Wohl et al., 2018). A careful analysis of wood flux pattern thus provides some potentially key insights about

614 the processes that prepare the stock of available wood within a reach and
615 should by the subject of further investigation.

616 Acknowledgments

617 We thank the Chinese Scholarship Council (CSC) PhD grant for Zhang.
618 This work was performed within the framework of the EUR H2O'Lyon (ANR-17-
619 EURE-0018) of Université de Lyon, within the program \Investissements
620 d'Avenir" operated by the French National Research Agency (ANR).

621 We would like to show our gratitude to Professor Lane, Dr. Kramer and one
622 anonymous reviewer, for their insights that helped us to enhance this work.

623 Data availability statement

624 Research data not shared.

625 References

626 Abbe TB, Montgomery DR. 2003. Patterns and processes of wood debris
627 accumulation in the Queets river basin, Washington. *Geomorphology* **51** (1-3):
628 81–107.

629 Ali I, Tougne L. 2009. Unsupervised Video Analysis for Counting of Wood
630 in River during Floods. *In Advances in Visual Computing,* Bebis G et al. (eds).
631 Springer Berlin Heidelberg: Berlin, Heidelberg; 578–587.

632 Belgiu M, Drăguţ L. 2016. Random forest in remote sensing: A review of
633 applications and future directions. *ISPRS Journal of Photogrammetry and*
634 *Remote Sensing* **114** : 24–31.

635 Benacchio V, Piégay H, Buffin-Bélanger T, Vaudor L. 2017. A new
636 methodology for monitoring wood fluxes in rivers using a ground camera:

637 Potential and limits. *Geomorphology* **279** : 44–58.

638 Benda L, Miller D, Sias J, Martin D, Bilby R, Veldhuisen C, Dunne T. 2003.
639 *In The Ecology and Management of Wood in World Rivers*, SV Gregory, KL
640 Boyer, AM Gurnell (eds). Symposium 37. American Fisheries
641 Society: Bethesda, MD; 49– 73.

642 Boivin M, Buffin-Bélanger T, Piégay H. 2015. The raft of the Saint-Jean
643 River, Gaspé (Québec, Canada): A dynamic feature trapping most of the wood
644 transported from the catchment. *Geomorphology* **231** : 270–280.

645 Braudrick CA, Grant GE, Ishikawa Y, Ikeda H. 1997. Dynamics of wood
646 transport in streams: a flume experiment. *Earth Surface Processes and*
647 *Landforms*: The Journal of the British Geomorphological Group **22** : 669–683.

648 Breiman L. 2001. Random Forests. Machine Learning **45** : 5–32.
649 Doi:10.1023/A:1010933404324

650 Comiti F, Andreoli A, Mao L, Lenzi MA. 2008. Wood storage in three
651 mountain streams of the Southern Andes and its hydro-morphological effects.
652 *Earth Surface Processes and Landforms* **33** (2): 244–262.

653 Comiti F, D'Agostino V, Moser M, Lenzi MA, Bettella F, Dell'Agnese A,
654 Rigon E, Gius S, Mazzorana B. 2012. Preventing wood-related hazards in
655 mountain basins: from wood load estimation to designing retention structures.
656 *Proceedings, 12th Congress INTERPRAEVENT 2012,* Grenoble, France; 651–
657 662.

658 Comiti F, Lucía A, Rickenmann D. 2016. Large wood recruitment and
659 transport during large floods: A review. *Geomorphology* **269** : 23–39.

660 De Cicco PN, Paris E, Ruiz-Villanueva V, Solari L, Stoffel M. 2018. In-
661 channel wood-related hazards at bridges: A review. *River Research and*
662 *Applications* **34** : 617–628.

663 Diehl TH. 1997. *Potential Drift Accumulation at Bridges*. Publication No.
664 FHWA - RD - 97 - 028. US Department of Transportation, Federal Highway
665 Administration, Research and Development, Turner - Fairbank Highway
666 Research Center: McLean, Virginia, USA.
667 http://www.tn.water.usgs.gov/pubs/FHWA-RD-97-028/drfront1.htm

668 Fischer M. 2006. Driftwood During the Flooding in Klosters in 2005, Report,
669 HSW Wädenswil, Switzerland (in German).

http://www.wsl.ch/fe/walddynamik/projekte/schwemmholzablagerungen/index_EN

Ghaffarian H, Lopez D, Mignot E, Piégay H, Rivière N. 2020b. Dynamics of floating objects at high particulate Reynolds numbers. *Physical Review Fluids* **5** (5): 054307.

Ghaffarian H, Piegay H, Lopez D, Rivière N, MacVicar B, Antonio A, Mignot E. 2020a. Video-monitoring of wood discharge: first inter-basin comparison and recommendations to install video cameras. *Earth Surface Processes and Landforms*. Available from: https://onlinelibrary.wiley.com/doi/abs/10.1002/esp.4875

Gippel CJ. 1995. Potential of turbidity monitoring for measuring the transport of suspended solids in streams. *Hydrological Processes* **9** (1): 83–97.

Gurnell A. 2012. Wood and river landscapes. *Nature Geoscience* **5** (2): 93–94.

Gurnell A, Petts G. 2006. Trees as riparian engineers: the Tagliamento river, Italy. *Earth Surface Processes and Landforms* **31** (12): 1558–1574.

Gurnell AM, Piégay H, Swanson FJ, Gregory SV. 2002. Large wood and fluvial processes. *Freshwater Biology* **47** (4): 601–619.

Hastie T, Tibshirani R, Friedman J. 2009. The elements of statistical learning: data mining, inference, and prediction. Springer Science & Business Media

Hutengs C, Vohland M. 2016. Downscaling land surface temperatures at regional scales with random forest regression. *Remote Sensing of Environment* **178** : 127–141.

Keller EA, Swanson FJ. 1979. Effects of large organic material on channel form and fluvial processes. *Earth Surface Processes* **4** (4): 361–380.

Kramer N, Wohl E. 2014. Estimating fluvial wood discharge using time-lapse photography with varying sampling intervals. *Earth Surface Processes and Landforms* **39** (6): 844–852.

Kramer N, Wohl E. 2017. Rules of the road: A qualitative and quantitative synthesis of large wood transport through drainage networks. *Geomorphology* **279** : 74–97.

Kramer N, Wohl E, Hess-Homeier B, Leisz S. 2017. The pulse of driftwood export from a very large forested river basin over multiple time scales, Slave River, Canada. *Water Resources Research* ***53*** (3): 1928–1947.

Lassettre NS, Kondolf GM. 2012. Large woody debris in urban stream channels: redefining the problem. *River Research and Applications* **28** (9): 1477–1487.

Lassettre NS, Piégay H, Dufour S, Rollet A-J. 2008. Decadal changes in distribution and frequency of wood in a free meandering river, the Ain River, France. *Earth Surface Processes and Landforms* **33** (7): 1098–1112.

Lemaire P, Piegay H, MacVicar B, Mouquet-Noppe C, Tougne L. 2014. Automatically monitoring driftwood in large rivers: preliminary results. *Presented at the 2014 AGU Fall Meeting*. 19 December, San Francisco, USA. Available from: https://agu.confex.com/agu/fm14/meetingapp.cgi/Paper/22487

Liaw A, Wiener M. 2002. Classification and Regression by RandomForest. **2** : 5.

Lyn D, Cooper T, Yi Y-K. 2003. Debris accumulation at bridge crossings: laboratory and field studies. Purdue University: West Lafayette. Available from: http://docs.lib.purdue.edu/jtrp/48

MacVicar B, Piégay H. 2012. Implementation and validation of video monitoring for wood budgeting in a wandering piedmont river, the Ain River (France). *Earth Surface Processes and Landforms* **37** (12): 1272–1289.

MacVicar B, Hauet A, Bergeron N, Tougne L, Ali I. 2012. River Monitoring with Ground-based Videography. *In Fluvial Remote Sensing for Science and Management,* PE Carbonneau, H Piégay (eds). Wiley: Chichester, UK; 367– 383.

MacVicar BJ, Piégay H, Henderson A, Comiti F, Oberlin C, Pecorari E. 2009. Quantifying the temporal dynamics of wood in large rivers: field trials of wood surveying, dating, tracking, and monitoring techniques. *Earth Surface Processes and Landforms* **34** (15): 2031–2046.

Mao L, Burns S, Comiti F, Andreoli A, Urciuolo A, Gaviño-Novillo M, Iturraspe R, Aristide Lenzi M. 2008. Acumulaciones de detritos leñosos en un cauce de montaña de Tierra del Fuego: análisis de la movilidad y de los efectos hidromorfológicos. Bosque (Valdivia) **29** : 197–211.

735 Marcus WA, Rasmussen J, Fonstad MA. 2011. Response of the Fluvial
736 Wood System to Fire and Floods in Northern Yellowstone. *Annals of the*
737 *Association of American Geographers* **101** (1): 21–44.

738 Martin DJ, Benda LE. 2001. Patterns of Instream Wood Recruitment and
739 Transport at the Watershed Scale. *Transactions of the American Fisheries*
740 *Society* **130** (5): 940–958.

741 Mazzorana B, Ruiz-Villanueva V, Marchi L, Cavalli M, Gems B, Gschnitzer
742 T, Mao L, Iroumé A, Valdebenito G. 2018. Assessing and mitigating large wood-
743 related hazards in mountain streams. *Journal of Flood Risk Management* **11**
744 (2): 207–222.

745 Mazzorana B, Zischg AP, Largiader A, Hübl J. 2009. Hazard index maps
746 for woody material recruitment and transport in alpine catchments. *Natural*
747 *Hazards and Earth System Sciences* **9** (1): 197–209.

748 Montgomery DR, Abbe TB, Buffington JM, Peterson NP, Schmidt KM,
749 Stock JD. 1996. Distribution of bedrock and alluvial channels in forested
750 mountain drainage basins. *Nature* **381** : 587–589.

751 Moulin B, Piegay H. 2004. Characteristics and temporal variability of large
752 woody debris trapped in a reservoir on the River Rhone(Rhone): implications
753 for river basin management. *River Research and Applications* **20** (1): 79–97.

754 Muste M, Fujita I, Hauet A. 2008. Large-scale particle image velocimetry
755 for measurements in riverine environments. *Water resources research* **44** (4):
756 W00D19.

757 Nakamura F, Swanson FJ. 1993. Effects of coarse woody debris on
758 morphology and sediment storage of a mountain stream system in western
759 Oregon. *Earth Surface Processes and Landforms* **18** (1): 43–61.

760 Piégay H, Moulin B, Hupp CR. 2017. Assessment of transfer patterns and
761 origins of in-channel wood in large rivers using repeated field surveys and wood
762 characterisation (the Isère River upstream of Pontcharra, France).
763 *Geomorphology* **279** : 27–43.

764 Ravazzolo D, Mao L, Picco L, Lenzi MA. 2015. Tracking log displacement
765 during floods in the Tagliamento River using RFID and GPS tracker devices.
766 *Geomorphology* **228** : 226–233.

767 Ruiz-Villanueva V, Bladé Castellet E, Díez-Herrero A, Bodoque JM,

768 Sánchez-Juny M. 2014a. Two-dimensional modelling of large wood transport
769 during flash floods. *Earth Surface Processes and Landforms* **39** (4): 438–449.

770 Ruiz-Villanueva V, Bürkli L, Mazzorana B, Mao L, Ravazzolo D, Iribarren P,
771 Wohl E, Nakamura F, Stoffel M. 2018. Defining and characterizing wood-laden
772 flows in rivers using home videos. In *E3S Web of Conference*, vol.40, p.02014.
773 EDP Sciences.

774 Ruiz-Villanueva V, Piégay H, Gurnell AM, Marston RA, Stoffel M. 2016a.
775 Recent advances quantifying the large wood dynamics in river basins: New
776 methods and remaining challenges: Large Wood Dynamics. *Reviews of*
777 *Geophysics* **54** (3): 611–652.

778 Ruiz-Villanueva V, Stoffel M, Piégay H, Gaertner V, Perret F. 2014b. Wood
779 density assessment to improve understanding of large wood buoyancy in rivers.
780 *River Flow 2014–Schleiss et Al.(Eds)* pp. 2503–2508.

781 Ruiz-Villanueva V, Wyżga B, Mikuś P, Hajdukiewicz H, Stoffel M. 2016b.
782 The role of flood hydrograph in the remobilization of large wood in a wide
783 mountain river. *Journal of Hydrology* **541** : 330–343.

784 Schenk ER, Moulin B, Hupp CR, Richter JM. 2014. Large wood budget and
785 transport dynamics on a large river using radio telemetry. *Earth Surface*
786 *Processes and Landforms* **39** (4): 487–498.

787 Senter A, Pasternack G, Piégay H, Vaughan M. 2017. Wood export
788 prediction at the watershed scale. *Earth Surface Processes and Landforms* **42**
789 (14): 2377–2392.

790 Seo JI, Nakamura F. 2009. Scale-dependent controls upon the fluvial
791 export of large wood from river catchments. *Earth Surface Processes and*
792 *Landforms* **34** (6): 786–800.

793 Seo JI, Nakamura F, Nakano D, Ichiyanagi H, Chun KW. 2008. Factors
794 controlling the fluvial export of large woody debris, and its contribution to
795 organic carbon budgets at watershed scales. *Water Resources Research* **44**
796 (4): W04428

797 Shields FD, Gippel CJ. 1995. Prediction of Effects of Woody Debris
798 Removal on Flow Resistance. *Journal of Hydraulic Engineering* **121** (4): 341–
799 354.

800 Team RC. 2019. R: A language and environment for statistical computing

(version 3.1. 2). Vienna, Austria.

Turowski JM, Badoux A, Bunte K, Rickli C, Federspiel N, Jochner M. 2013. The mass distribution of coarse particulate organic matter exported from an alpine headwater stream. *Earth Surface Dynamics Discussions* **1** (1): 1–29.

Waldner P, Rickli C, Köchlin D, Usbeck T, Schmocker L, Sutter F. 2007. Schwemmholz. Ereignisanalyse Hochwasser 2005–Teil 1: Prozes se, Schäden und erste Einordnung (in German). Bundesamt für Umwelt BAFU, *Eidgenössische Fors chungsanstalt WSL*. Bezzola GR, Hegg C. Umwelt-Wissen **825** : 181–193.

Wilcox AC, Wohl EE. 2006. Flow resistance dynamics in step-pool stream channels: 1. Large woody debris and controls on total resistance. *Water Resources Research* **42** (5):W05418.

Wohl E. 2013. Floodplains and wood. *Earth-Science Reviews* **123** : 194–212.

Wohl E, Cadol D, Pfeiffer A, Jackson K, Laurel D. 2018. Distribution of large wood within river corridors in relation to flow regime in the semiarid western US. *Water Resources Research* **54** (3): 1890–1904.

Young WJ. 1991. Flume study of the hydraulic effects of large woody debris in lowland rivers. *Regulated Rivers: Research & Management* **6** (3): 203–211.

Yue S, Ouarda TBMJ, Bobée B, Legendre P, Bruneau P. 1999. The Gumbel mixed model for flood frequency analysis. *Journal of Hydrology* **226** (1): 88–100.